The influence of microscopic disorder on electron paramagnetic resonance spectra of Eu^{2+} ions in $Pb_{1-x}Ge_xTe$

2009 J. Phys.: Condens. Matter 21 405802

(http://iopscience.iop.org/0953-8984/21/40/405802)

J. Phys.: Condens. Matter **21** (2009) 405802 (6pp) doi:10.1088/0953-8984/21/40/405802

The influence of microscopic disorder on electron paramagnetic resonance spectra of Eu^{2+} ions in $Pb_{1-x}Ge_xTe$

T Radzyński, A Łusakowski, K Świątek and T Story

Institute of Physics, Polish Academy of Sciences, Aleja Lotników 32/46, 02-668 Warsaw, Poland

E-mail: radzy@ifpan.edu.pl

Received 25 May 2009, in final form 14 August 2009
Published 17 September 2009
Online at stacks.iop.org/JPhysCM/21/405802

Abstract

In mixed crystals, because of the different ionic radii of cations or anions and the randomness in the placement of ions of different kinds, the crystal lattice is locally deformed. Such local deformations have significant influence on the ground state splitting of magnetic ions. Because this ground state splitting is responsible for the position of the electron paramagnetic resonance (EPR) lines, microscopic disorder is one of the factors which lead to the broadening of the lines, and eventually to their disappearance. This paper is devoted to semi-quantitative analysis of the influence of microscopic disorder on EPR spectra. The theory is compared against measurements performed on mono-crystalline $Pb_{1-x}Ge_xTe$ epitaxial layers containing Eu^{2+} ions for different germanium and europium contents. With increasing germanium content we observe gradual disappearance of the EPR lines, although macroscopically, on the basis of x-ray diffraction analysis, each layer might have been considered as a perfect crystal.

1. Introduction

In mixed crystals we have at least two, or in general more, different average cation–anion distances. For example in the substitutional solid solution $A_{1-x}B_xC$ we expect two average distances, d_{A-C} and d_{B-C}, between anion C and the two cations A and B. The average distances between ions in mixed crystals are measured using the extended x-ray absorption fine structure analysis (EXAFS) technique. Sometimes the situation may be much more complicated, like in the case of IV–VI semiconductor $Pb_{1-x}Ge_xTe$ crystals, where due to the structural transition from cubic to rhombohedral structure and the non-symmetrical placement of germanium atoms in elementary cells, there are three different distances between tellurium and germanium [1]. The presence of different cation–anion distances together with the random placement of different cations in the crystal lattice inevitably leads to microscopic disorder. This means that the directions of bonds and their lengths are deflected from the directions and lengths in a perfect lattice. Consequently, the symmetry of the nearest neighbourhood of an ion is lowered. Calculations show that such a lowering of the symmetry has a significant influence on the ground state splitting of magnetic ions and, as will be shown below, also on the width of lines and the decay of their amplitudes in electron paramagnetic resonance (EPR) spectra. Showing this correspondence between microscopic disorder and EPR spectra is the main aim of the present paper.

We theoretically and experimentally study microscopic disorder in a model system of $Pb_{1-x}Ge_xTe$ semiconductor mixed crystals doped with S-state Eu^{2+} ions. The main ideas of this work apply to the broad class of magnetically doped crystals. We present EPR spectra for five epitaxial layers of $Pb_{1-x-y}Ge_xEu_yTe$ of high crystal quality. The main differences between the layers were in the contents of germanium and europium [2]. These contents were designed to provide strong enough Eu^{2+} EPR signals for the layers, $y \geqslant 1\%$, and by changing the germanium content, $0 \leqslant x \leqslant 0.164$, to control the degree of microscopic disorder. This disorder rapidly grows with increasing germanium content because of the large difference between the ionic radii of Pb and Ge. In the following sections we show experimental results of EPR measurements and after introducing a quantitative measure of the degree of microscopic disorder and a short description of the main mechanism leading to the ground state splitting of europium ions, we discuss the relation between microscopic disorder and the Eu^{2+} fine structure EPR lines. Results of

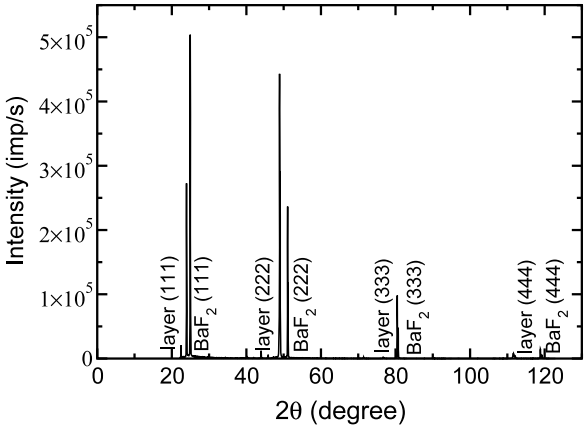

Figure 1. XRD spectrum measured for $Pb_{1-x-y}Ge_xEu_yTe/BaF_2$ layers with $x = 0.049$ and $y = 0.011$.

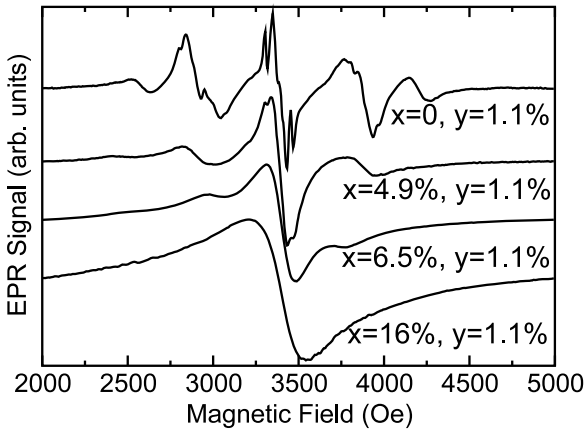

Figure 2. EPR power absorption derivatives for Eu^{2+} ion in $Pb_{1-x-y}Ge_xEu_yTe$ for different Ge concentrations. The external magnetic field is along the [001] crystallographic direction.

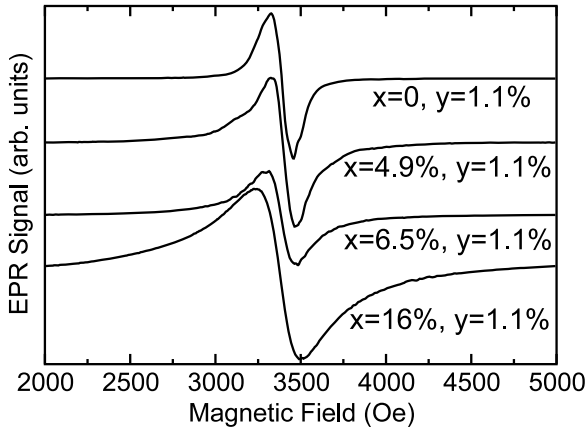

Figure 3. EPR power absorption derivatives for Eu^{2+} ion in $Pb_{1-x-y}Ge_xEu_yTe$ for different Ge concentrations. The external magnetic field is along the [112] crystallographic direction.

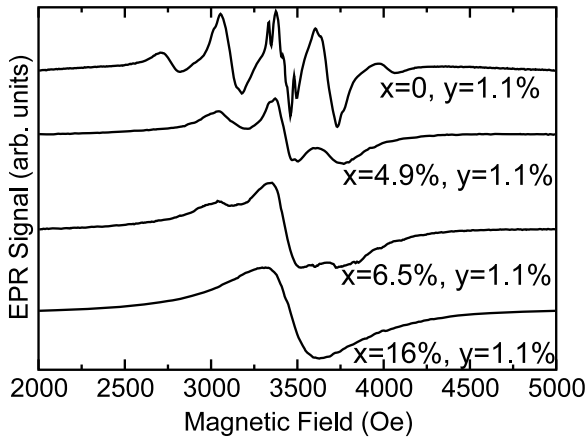

Figure 4. EPR power absorption derivatives for Eu^{2+} ion in $Pb_{1-x-y}Ge_xEu_yTe$ for different Ge concentrations. The external magnetic field is along the [111] crystallographic direction.

calculations will be compared to the results of measurements for layers of $Pb_{1-x-y}Ge_xEu_yTe$.

As regards the theoretical part of the paper, some ideas were already introduced and described in our previous works, but in a different context—explanation of the magnetic specific heat of $Pb_{1-x}Eu_xTe$ [3] and of the magnetic anisotropy of $Pb_{1-x-y}Sn_xMn_yTe$ [4]. In papers [3, 5, 6], discussing the mechanisms of the ground state splitting we pointed out the important role played by the 5d levels of rare earth ions. That is why, presenting the mechanism of the ground state splitting for europium ions, we sketch the main assumptions only, referring the reader to [3] for details.

2. Experiment

We measured EPR spectra for five samples of $Pb_{1-x-y}Ge_xEu_yTe$ layers grown on the $BaF_2(111)$ substrate by a molecular beam epitaxy (MBE) method employing effusion cells for PbTe, GeTe, Eu and Te. In four samples the content of europium was $y = 0.011$ and the contents of germanium were $x = 0$, 0.049, 0.065 and 0.164. In the fifth sample $x = 0.046$ while the europium content $y = 0.044$ was significantly larger than in the first four samples. $Pb_{1-x-y}Ge_xEu_yTe$ grows on $BaF_2(111)$ substrate epitaxially along the [111] direction. The thicknesses of the layers were of the order of 1 μm; thus we expected the layers to be crystallographically relaxed and the crystal structure to behave like that of bulk crystals. It is known that PbTe has rock salt structure and the structure of $Pb_{1-x}Ge_xTe$ depends on the chemical composition and temperature [1]. At high temperatures it has rock salt structure and below a certain temperature which depends on the germanium content there is a structural transition to the rhombohedral structure with the angle defining the structure, $\alpha \approx 89°$ as compared to $\alpha = 90°$ for rock salt. Each layer was analysed by the x-ray diffraction (XRD) method. From this analysis one draws the conclusion that all the samples were homogeneous, high quality crystal layers. In figure 1 we present XRD spectra for one of the samples studied. For other samples the spectra look similar.

The EPR spectra of $Pb_{1-x-y}Ge_xEu_yTe$ were measured in the temperature range 5–300 K using an X-band Brucker spectrometer operating at frequency 9.46 GHz. The spectra at $T = 5$ K for the external magnetic field applied along different crystallographic directions for samples with the same Eu content of 1.1 at.% are presented in figures 2–4. For the

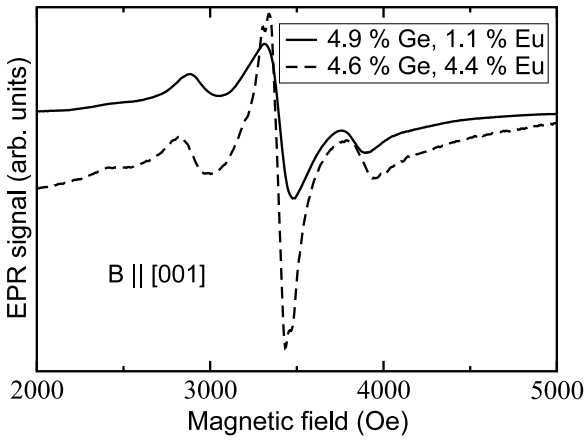

Figure 5. Comparison of EPR power absorption derivatives for two samples $Pb_{1-x-y}Ge_xEu_yTe$: $x = 0.049$, $y = 0.011$ and $x = 0.046$, $y = 0.044$ for the magnetic field along the [001] direction.

best resolved spectrum of PbTe:Eu, $x = 0$, with the magnetic field applied along the [001] direction, the expected seven-line fine structure pattern is observed due to the ligand crystal field. For other directions, lines overlap, because their positions depend on the direction of the external magnetic field [7]. The additional splittings observed experimentally are due to hyperfine coupling between the electron spin of the 4f shell and the europium nuclear spin. In figure 5 we compare EPR spectra for the external magnetic field along the [001] direction for two samples with similar contents of germanium and significantly differing contents of Eu. Inspecting figures 2–4 one may clearly note a gradual decay of the EPR lines' amplitudes with increasing germanium content. On the other hand, figure 5 shows that the spectra are much less influenced by changes of europium content. In the literature the decay of the EPR lines' amplitudes due to broadening of the lines is often attributed to random magnetic fields due to long range Eu–Eu dipole–dipole interaction. The effect of this mutual interaction should grow with increasing Eu content in the crystal. Inspecting figures 2–5 one may notice that the change of germanium content from 4.9% to 6.5% has much larger influence on the EPR spectra than the change of europium content from 1.1% to 4.4%. The lattice constants for PbTe, EuTe and GeTe are 6.462 Å, 6.598 Å and 5.996 Å, respectively [14, 1]. Thus, we expect for $Pb_{1-x-y}Ge_xEu_yTe$ the difference between the lengths of Pb–Te and Ge–Te bonds to be significantly larger than the difference between the Eu–Te and Pb–Te bonds' lengths. That is why we expect the presence of germanium in PbTe to cause much larger microscopic disorder than the presence of europium. We think that figures 2–5 support the statement mentioned in the introduction that the microscopic disorder influences EPR spectra. Below, we show this semi-quantitatively using a simple model of the disorder and one of the possible mechanisms of ground state splitting for Eu ions.

3. A measure of microscopic disorder

$Pb_{1-x}Ge_xTe$ with x of the order of a few per cent exists in two crystal structures. At high temperatures it possesses rock salt structure, and below a certain temperature, which depends on the germanium content, it has rhombohedral structure which can be viewed as a small elongation of the cube along the [111] diagonal with the change of the angle $\alpha = 90°$ to $\approx 89°$. The europium ions introduced into the PbGeTe crystal are expected to replace lead or germanium ions. For the reasons discussed in the introduction the nearest neighbourhood of Eu, which is formed by six tellurium ions, is deformed compared to the perfect rhombohedral symmetry case. In our model description of disorder we assume that the directions of Eu–Te bonds are distributed around corresponding crystallographic directions in a perfect rhombohedral lattice. More precisely, let us put the origin of the coordinate system at the position of the europium ion and the z axis along the Eu–Te bond in the perfect rhombohedral lattice. Then the bond's direction in the disordered lattice may be specified by two angles, θ and φ. In our model of disorder it is assumed that these angles are random variables. The angle θ is a positive, Gaussian distributed variable with variance θ_0 and φ is homogeneously distributed between 0 and 2π. In this simple description we neglect possible random changes of Eu–Te bond lengths, correlations between directions of neighbouring bonds, which should be taken into account in a more realistic model.

For a given configuration of six neighbouring tellurium atoms it is possible to calculate the crystal field potential

$$V_{\mathrm{cr}}(\mathbf{r}) = \sum_{l=0}^{\infty} \sum_{m=-l}^{l} A_{lm} \left(\frac{r}{r_0}\right)^l C_{lm}(\theta, \varphi) \tag{1}$$

for the Eu ion. In equation (1) $r_0 = 0.529$ Å is the atomic length unit and the functions $C_{lm}(\theta, \varphi)$ are related to spherical harmonics by the equation $C_{lm}(\theta, \varphi) = (4\pi/(2l + 1))^{1/2} Y_{lm}(\theta, \varphi)$. In the simple model the crystal field potential is produced by six point charges Ze placed at $(r_i \theta_i \varphi_i)$, $i = 1, \ldots, 6$. Then the coefficients A_{lm} are equal to

$$A_{lm} = Ze^2 \sum_{i=1}^{6} \frac{r_0^l}{r_i^{l+1}} C^*_{lm}(\theta_i, \varphi_i), \tag{2}$$

where the star denotes the complex conjugate. The crystal field potential of equation (1) is used in calculations of the effective spin Hamiltonian for the Eu ion.

4. The effective spin Hamiltonian for the Eu ion

In IV–VI semiconductors the europium ion usually is in the configuration Eu^{2+} and has seven electrons on the 4f shell. These electrons are responsible for the magnetic moment of the ion. According to Hund's rule, for this electron configuration, the ground state should be characterized by the total orbital angular momentum $L = 0$ and the total spin $S = 7/2$. This means that the ground state should be $^8S_{7/2}$, an eightfold-degenerate state, and as an entity with $L = 0$ it should not interact with the crystal environment. Such a picture explains quite well experiments in which the magnetic susceptibility or magnetization in semimagnetic (diluted magnetic) semiconductors is studied. However other experiments, like magnetic specific heat measurements [3] and

particularly EPR measurements, which are the main topic of the present paper, clearly show that actually the ground state of Eu^{2+} ion is not eightfold degenerate but split. The splitting is caused by a crystal environment and may be described qualitatively using an effective spin Hamiltonian [7]. For perfect cubic symmetry it has the form

$$H^{\mathrm{cub}} = \frac{b_4}{60}(O_4^0 + 5O_4^4) + \frac{b_6}{1260}(O_6^0 - 21O_6^4) \tag{3}$$

where b_4 and b_6 are coefficients and the operator equivalents O_k^m are 8×8 matrices defined in [7]. If the symmetry of the ion's neighbourhood is lower, one should add to the Hamiltonian additional terms. There are different causes of symmetry lowering. One of them is the lattice mismatch between compounds forming the layer and the substrate. For example for thin films of $Pb_{1-x-y}Ge_xEu_yTe$ grown on BaF_2 substrate the additional term reads

$$H^{\mathrm{trig}} = b_2(S_xS_y + S_yS_z + S_zS_x + \mathrm{h.c.}) \tag{4}$$

where S_x, S_y and S_z are spin operators (the abbreviation h.c. means Hermitian conjugate). The form of H^{trig} is dictated by the experimental fact that the layer of $Pb_{1-x}Ge_xTe$ grows on BaF_2 substrate in the [111] direction. Let us note that the Hamiltonians in equations (3) and (4) contain only terms which may be expressed as even powers of spin operators. This is connected with time reversal symmetry which the Hamiltonian should obey in the absence of an external magnetic field. In general, an 8×8 complex Hermitian, traceless matrix obeying time reversal symmetry may be expressed as a certain combination of 28 independent Hermitian matrices, $\sum_{i=1}^{28} a_i h_i$. The general formulae for h_i may be found in [8]. Here we write only matrices which may be expressed as second powers of spin operators and, as regards symmetry properties, are analogues of real combinations of spherical harmonics Y_{lm} with $l = 2$:

$$\begin{aligned} h_1 &= \frac{1}{\sqrt{12}}(3S_z^2 - 63/4) \qquad h_2 = \tfrac{1}{2}(S_x^2 - S_y^2) \\ h_3 &= \tfrac{1}{2}(S_xS_y + S_yS_x) \qquad h_4 = \tfrac{1}{2}(S_yS_z + S_zS_y) \\ h_5 &= \tfrac{1}{2}(S_zS_x + S_xS_z). \end{aligned} \tag{5}$$

Our calculations showed that these terms have the largest influence on the ground state splitting of the europium ion; the terms containing higher powers of spin operators have much smaller effects. Thus for an arbitrarily deformed environment of the Eu ion we add to the effective spin Hamiltonian the term

$$\Delta H = \sum_{i=1}^{5} a_i h_i. \tag{6}$$

The problem of calculation of the coefficients b_2, b_4 and b_6 for rare earth ions is very old. In the literature there exist many papers devoted to that topic [9–12, 5]. There is no consensus in the literature concerning the mechanism leading to parameters describing the ground state splitting of $^8S_{7/2}$ ions, in particular europium ones. There is no general method enabling precise calculations of these parameters for an ion in an arbitrary crystal. In practice b_2, b_4 and b_6 are treated as fitting parameters and the main conclusion drawn from EPR experiments is information about the symmetry of the ion's neighbourhood. Calculations may only give orders of magnitude for these parameters.

In [3] we analysed and estimated the relative importance of several mechanisms leading to the ground state splitting of Eu^{2+} ions in disordered environments in PbTe bulk crystal. From this analysis it turned out that the most important mechanism is based on $4f^7 \leftrightarrow 4f^6 5d^1$ virtual transitions caused by the crystal field potential. The method of calculation of the effective spin Hamiltonian is described in detail in [3]; here we only describe the main idea.

The basis of the Hamiltonian consists of eight degenerate ground states of the term $^8S_{7/2}$ and 490 excited states of the configuration $4f^6 5d^1$. The Hamiltonian describing the excited states reads

$$H_{4f^6 5d^1} = H_{4f^6} + \lambda_{5d}\mathbf{l}\cdot\mathbf{s} - J_{fd}\mathbf{S}\cdot\mathbf{s} + V_{\mathrm{cr}} + \epsilon_0 \tag{7}$$

where

$$H_{4f^6} = \lambda_{4f}\mathbf{L}\cdot\mathbf{S} + \lambda_{4f}^1(\mathbf{L}\cdot\mathbf{S})^2 \tag{8}$$

describes the spin–orbit interaction for six electrons on the 4f shell. It is assumed that Hund's rule does apply for six 4f electrons; thus the total orbital angular momentum $L = 3$ and the total spin $S = 3$. The other terms on the right-hand side of equation (7) are responsible for the spin–orbit interaction on the 5d shell, the exchange interaction between 5d and 4f electrons, the crystal field potential acting on 5d states and the energy necessary to transfer an electron from a 4f to a 5d shell. There are 490 states for the configuration $4f^6 5d^1$. The $4f^7 \leftrightarrow 4f^6 5d^1$ transitions between ground and the excited states are caused by the crystal field potential. A more detailed discussion and the values of the parameters for the Hamiltonian appear in [3].

For a particular configuration of six tellurium ions, after solving the eigenproblem for the resulting 498×498 Hamiltonian matrix it is possible to construct an effective spin Hamiltonian matrix. Next, performing its decomposition in the basis we obtain coefficients a_i, equation (6), for the particular configuration of the europium ion's neighbourhood.

Let us stress that the mechanism described above is only one among a number of mechanisms possibly responsible for the ground state splitting. According to the analysis performed [3], it leads to the largest ground state splittings; thus it should also significantly influence the EPR spectra. However it certainly does not give, for example, the coefficients b_2, b_4 and b_6 measured in experiments. This is connected with the fact that the matrix elements connecting ground and excited states contain factors $\langle\phi_m^{5d}|V_{\mathrm{cr}}|\phi_M^{4f}\rangle$ where ϕ_m^{5d} $(-2 \leqslant m \leqslant 2)$ and ϕ_M^{4f} $(-3 \leqslant M \leqslant 3)$ are 5d and 4f orbitals, respectively [3]. Because of the opposite parity of these orbitals, in the crystal field potential, equation (1), only terms with odd l influence the matrix elements $\langle\phi_m^{5d}|V_{\mathrm{cr}}|\phi_M^{4f}\rangle$ and those with even l, which are of primary importance for cubic or homogeneously deformed crystals, are not taken into account.

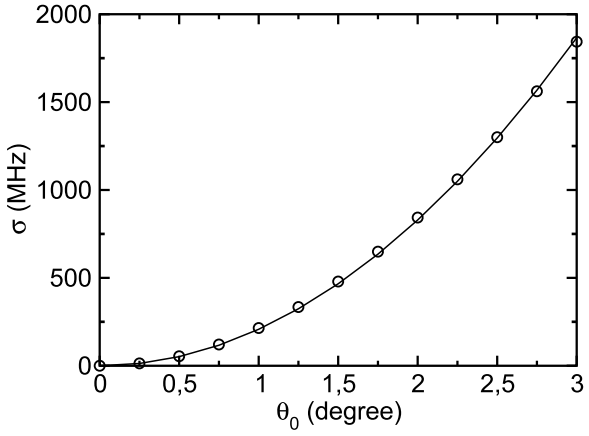

Figure 6. The dependence between parameters describing the randomness of the Hamiltonian and the disorder.

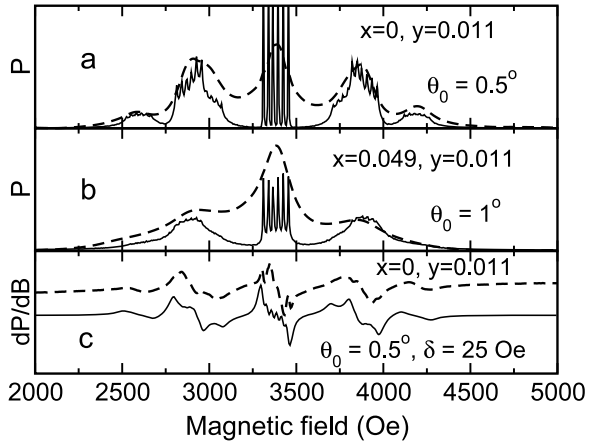

Figure 7. ((a), (b)) Integrated EPR power absorption derivative; (c) EPR power absorption derivative for Eu^{2+} ions in $Pb_{1-x-y}Ge_xEu_yTe$. Broken lines—experiment; continuous lines—theory. All curves are for magnetic field parallel to the [001] crystallographic direction.

5. Results and conclusions

In order to obtain stochastic properties of the crystal field Hamiltonian we generated 10 000 random configurations of europium neighbourhoods for several values of θ_0 and for each configuration, using the method described above, we calculated the coefficients a_i, equation (6). Further analysis shows that for each θ_0 the coefficients a_i are independent random variables with zero mean and a dispersion which grows with the disorder measure, θ_0, like θ_0^2. In figure 6 we show calculated points and the fitted relation $\sigma \equiv \sqrt{\langle a_i^2 \rangle} \approx c\theta_0^2$ where the coefficient $c = 207$ MHz.

Figures 7(a) and (b) show the influence of microscopic disorder on the EPR spectrum. The broken curves are EPR power absorption spectra obtained from experimental data presented in figures 2 by integration. In order to obtain corresponding theoretical curves we start with the Hamiltonian

$$H = g\mu_B \mathbf{B}\cdot\mathbf{S} + A\mathbf{S}\cdot\mathbf{I} + H^{\text{cub}} + H^{\text{trig}} \qquad (9)$$

where H^{cub} and H^{trig} are defined by equation (3) and equation (4), respectively. In equation (9) we included Zeeman and hyperfine terms [7]. The values for the g-factor, $g = 1.982$, and hyperfine constant, $A = 80$ MHz, describing the exchange interaction between the spin of the 4f shell and the spin $I = 5/2$ of the Eu nucleus were obtained from EPR spectra for Eu in PbTe [13]; we expect them not to differ significantly for $Pb_{1-x}Ge_xTe$. The best agreement between positions of theoretical EPR lines resulting from the Hamiltonian, equation (9), and experimental data for the sample without germanium, $x = 0$, were obtained for $b_4 = 113$ MHz, $b_6 = -3$ MHz and $b_2 = -13$ MHz. The nonzero value for b_2 clearly indicates that although the measured layers are rather thick, of the thickness 1 μm, and thus they should be relaxed and the europium ions' neighbourhoods should possess O_h symmetry, there remain certain global deformations. We think that these deformations are caused by the substrate because they exist even for a germanium free sample. Similar deformations were observed for PbTe:Eu grown on a KCl(001) substrate; in that case the layer grew in the [001] direction. The values for b_4 and b_6 for PbTe:Eu/BaF_2 are of the same order of magnitude as those found for Eu^{2+} in the PbTe layer grown on a KCl substrate—for PbTe:Eu/KCl, $b_4 = 120$ MHz and $b_6 = -3$ MHz [13]. As was shown in [5], the value of the parameter b_4 is very sensitive to the details of the band structure and the position of the atomic 5d level of europium with respect to the Fermi level. Thus the differences between the values for parameter b_4 for different samples are not related to an experimental error or erroneous interpretation of the experimental results but rather reflect small differences between samples, for example different thermal strains (originating from thermal expansion coefficient mismatch between the layer and BaF_2 or KCl substrates) or different carrier concentrations.

In order to take into account microscopic disorder for a given θ_0, using a random number generator, we generated 10 000 configurations of europium's neighbourhoods. Let c be an index numbering these configurations. For each c we calculated Hamiltonian ΔH^c according to the procedure described in the previous section. After adding ΔH^c to the Hamiltonian in equation (9) and choosing the magnetic field direction, we calculated the dependence of the energy levels on the value of the external magnetic field B. The knowledge of this dependence enabled us to find the magnetic fields B_i^c for which the EPR resonance condition was satisfied. Applying the Fermi golden rule we calculated corresponding intensities A_i^c of the transitions. The index i ($1 \leqslant i \leqslant 252$) numbers the transitions for a configuration c. Without the hyperfine interaction, in general, we would have seven resonance fields. However, due to the hyperfine interaction each energy level of an ion is split into six levels. Thus, instead of one, there are $6 \times 6 = 36$ possible resonance fields and consequently for each configuration there are $7 \times 36 = 252$ possible transitions. After the calculation of B_i^c and A_i^c we divided the interval (2000, 5000 Oe) into 500 equal intervals (b_J, b_{J+1}) where $J = 0, \ldots, 499$. Next, for each interval we calculated $A_J = \sum_{c,i}^{J} A_i^c$ where the symbol $\sum_{c,i}^{J}$ denotes the sum over those c, i for which we have that the magnetic fields $B_i^c \in$

(b_J, b_{J+1}). In this way we obtained the histograms presented in figures 7(a) and (b) (continuous lines). Let us note that in figures 7(a) and (b) we present a power spectrum, not its derivative with respect to B. The reason is that a histogram is not a differentiable function of B and it would be necessary to apply some smoothing procedure which is not unique.

We see that in accordance with the experiment, the increase of the disorder level (increase of θ_0) leads to the lines broadening and disappearance of the side lines. For larger values of the disorder parameter θ_0, for $\theta_0 > 2.5°$ we obtain the central line only.

On the other hand, contrary to the case for experimental results, the central line, according to the present theory, is only weakly influenced by the microscopic disorder and even for $\theta_0 = 1°$ the superfine structure is clearly visible. This is caused by the fact that the position of this line is very weakly influenced by additional terms in the Hamiltonian. This leads to the conclusion that the microscopic disorder is not the only cause of the line broadening, and other mechanisms should be taken into account. In order to simulate the other mechanisms, we assume that lines $\{c, i\}$, instead of being Dirac like delta functions, are broadened according to the Lorentz formula. This means that we assume that the power absorption spectrum is proportional to

$$P(B) = \sum_{c,i} \frac{A_i^c}{(B - B_i^c)^2 + \delta^2} \tag{10}$$

where δ describes the broadening. Unlike the histogram, function $P(B)$ is a differentiable function of the magnetic field B. The resulting power absorption derivative is compared to the experimental data in figure 7(c). The theoretical curve was obtained for $\theta_0 = 0.5°$ and $\delta = 25$ Oe. This value of δ is close to $\delta = 20$ Oe, obtained for PbTe:Eu/KCl [13].

In conclusion, comparing the theoretical prediction with the experimental data we explicitly showed that the microscopic disorder is one of the important mechanisms which should be taken into account when analysing the broadening of EPR lines and the decay of their amplitudes. Our simulations show that the fastest decay, consistently with experiment, is observed for the non-central fine structure split EPR lines. The central line is influenced by the microscopic disorder last. This is connected with the fact that the position of this line is very weakly influenced by additional terms in the Hamiltonian. That is why the sharp peaks originating from hyperfine coupling are seen in figure 7 for the central line even for larger disorder, while they are practically invisible for the side lines. These sharp peaks disappear if we assume that there exist other mechanisms leading to the broadening of the lines which are not related to the microscopic disorder.

Finally our measurements and the resulting nonzero parameter b_2 clearly indicate that even for a germanium free sample the layers are not fully relaxed; there are strains due to substrate–layer lattice or thermal mismatch.

Acknowledgments

This work was supported by the research project No. 0992/T02/2007/32, granted for the period 2007–2010 by the Ministry of Science and Higher Education (Poland). We would like to acknowledge P Dziawa and B Taliashvili for the growth of the layers and V Domukhovski for XRD structure characterization.

References

[1] Ravel B, Cockayne E, Newville M and Rabe K M 1999 *Phys. Rev.* B **60** 14632
[2] Osinniy V, Dziawa P, Domukhovski V, Dybko K, Knoff W, Radzyński T, Łusakowski A, Świątek K, Łusakowska E, Taliashvili B, Boratyński A and Story T 2008 *Narrow Gap Semiconductors* (*Springer Proceedings in Physics*) vol 119 (Berlin: Springer) p 73
[3] Górska M, Łusakowski A, Jędrzejczak A, Gołacki Z, Gałązka R R, Anderson J R and Balci H 2006 *Phys. Rev.* B **73** 125201
[4] Łusakowski A 2006 *Solid State Commun.* **137** 107
[5] Łusakowski A 2005 *Phys. Rev.* B **72** 094429
[6] Łusakowski A, Górska M, Anderson J R, Dagan Y and Gołacki Z 2009 *J. Phys.: Condens. Matter* B **21** 265802
[7] Abragam A and Bleaney B 1970 *Electron Paramagnetic Resonance of Transition Ions* (Oxford: Clarendon)
[8] Judd B R 1963 *Operator Techniques in Atomic Spectroscopy* (New York: McGraw-Hill)
[9] Wybourne B G 1966 *Phys. Rev.* **148** 317
[10] Barnes S E, Baberschke K and Hardiman M 1978 *Phys. Rev.* B **18** 2409
[11] Newman D J and Urban W 1975 *Adv. Phys.* **24** 793
[12] Smentek L, Wybourne B G and Kobus J 2001 *J. Phys. B: At. Mol. Opt. Phys.* **34** 1513
[13] Fedorych O and Łusakowski A 2004 unpublished
[14] Kepa H, Springholz G, Giebultowicz T M, Goldman K I, Majkrzak C F, Kacman P, Blinowski J, Holl S, Krenn H and Bauer G 2003 *Phys. Rev.* **68** 024419